Systematic Investigation on the Formation of Honeycomb-Patterned Porous Films from Amphiphilic Block Copolymers

ARTICLE *in* THE JOURNAL OF PHYSICAL CHEMISTRY C · JANUARY 2015

Impact Factor: 4.77 · DOI: 10.1021/jp5119212

6 AUTHORS, INCLUDING:

Bai-Heng Wu
Zhejiang University
2 PUBLICATIONS **13** CITATIONS
SEE PROFILE

Liangwei Zhu
Zhejiang University
11 PUBLICATIONS **126** CITATIONS
SEE PROFILE

Yang Ou
State Key Laboratory of Resources and Enviro…
67 PUBLICATIONS **527** CITATIONS
SEE PROFILE

Zhi-Kang Xu
Zhejiang University
251 PUBLICATIONS **6,271** CITATIONS
SEE PROFILE

THE JOURNAL OF PHYSICAL CHEMISTRY C

Article

pubs.acs.org/JPCC

Systematic Investigation on the Formation of Honeycomb-Patterned Porous Films from Amphiphilic Block Copolymers

Bai-Heng Wu, Liang-Wei Zhu, Yang Ou, Wen Tang, Ling-Shu Wan,* and Zhi-Kang Xu

MOE Key Laboratory of Macromolecular Synthesis and Functionalization, Department of Polymer Science and Engineering, Zhejiang University, Hangzhou 310027, People's Republic of China

Supporting Information

ABSTRACT: The breath figure method is a very simple and highly efficient technique to prepare honeycomb-patterned porous structures. Amphiphilic block copolymers are the most used film-forming materials. However, the relationship between block copolymer composition and film morphology is still unknown, which hinders the large-scale fabrication of the films. In this work, we synthesized more than 30 amphiphilic block copolymers with different chemical compositions by atom transfer radical polymerization (ATRP). Honeycomb films were prepared from polystyrene-*block*-poly(*N*,*N*-dimethylaminoethly methacrylate) (PS-*b*-PDMAEMA) by the breath figure method. An empirical morphology diagram was obtained to show the relationship between the block copolymer composition and the film-forming ability, in which zones corresponding to large-area ordered, ordered, partially ordered, and disordered films have been revealed. Moreover, interfacial tensions of these copolymers were measured by a pendant drop method. A polymerization degree ratio of PDMAEMA block to PS block between 0.01 and 0.02, which has interfacial tensions in the range of 34.5−46.0 mN/m, is favorable for the preparation of ordered honeycomb films. For polystyrene-*block*-poly(2-hydroxyethyl methacrylate) (PS-*b*-PHEMA) that has a more hydrophilic block than PS-*b*-PDMAEMA, it may form reverse micelles in solutions and hence shows different interfacial tensions and self-assembling behaviors when the PHEMA block is long. This study unveils the relationship between block copolymer composition and honeycomb film morphology and provides new insights into designing polymers for large-area, highly ordered, and reproducible honeycomb-patterned porous films.

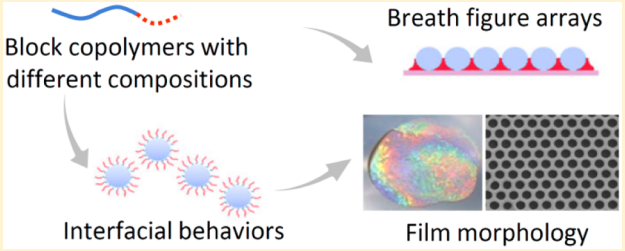

INTRODUCTION

Well-ordered films with micrometer- or nanometer-sized pores have attracted much attention due to the wide range of potential applications, such as templating materials,[1−4] microcontainers,[5,6] superhydrophobic surfaces,[7] separation membranes,[8−11] sensing materials,[12] biomaterials,[13−16] and photoelectronic materials.[17−20] The breath figure method was invented by Widawski et al. in 1994.[21] When a polymer solution is cast onto a substrate under a humid airflow, solvent evaporates and results in temperature reduction, which facilitates condensation and growth of water droplets. At the same time, polymer concentrates at the interface to stabilize the water droplets. With the help of Marangoni convection and thermocapillary effect, the water droplets arrange into close-packed hexagonal arrays. Along with further evaporation of the solvent and water, pores are shaped by the water droplets, and honeycomb-patterned films could be obtained. Compared with traditional top-down patterning techniques, the breath figure method shows many advantages, such as time-saving, energy-saving, environmentally friendly, and versatililty to many materials.

It has been reported that the structures of honeycomb-patterned porous films, such as pore size, pore shape, and multilayer structures, could be affected by a series of factors, which include air flow rate, solvent property, relative humidity, solution concentration, substrates, and polymer architectures.[22−25] Among them, polymer architectures play a decisive role in the morphologies of the films. Since star-shaped polymers were first reported to be used to fabricate porous films,[21,26] polymers with different architectures such as comb-like polymers,[27,28] rod−coil block copolymers,[29,30] linear polymers with or without polar end groups,[27] and amphiphilic block copolymers[28,31−34] have been verified for the formation of honeycomb-patterned porous films. For hydrophobic star-shaped polymers, the ability to generate films with a high degree of ordering is related to their ability to precipitate instantaneously at the solution/water interface. Stenzel et al. found that the pore size dramatically decreases when the number of the arms of the star polymers increases,[26] which is attributed to the increased ability of the polymers to stabilize water droplets. Linear polymers without polar moieties are able to form well-ordered honeycomb films only under specific conditions such as in a specific solvent[35] or a relatively high concentration (generally higher than 10 mg/mL).[36] It has been

Received: November 30, 2014
Revised: December 29, 2014
Published: January 7, 2015

DOI: 10.1021/jp5119212
J. Phys. Chem. C 2015, 119, 1971−1979

accepted that the polar moieties of linear polymers have marked influences on film morphologies. As an example, introducing polar end groups to polystyrene improves the film-forming property,[37,38] which confirms the importance of the polar composition of a polymer to the stabilization of condensed water droplets.

Amphiphilic block copolymers composed of hydrophilic and hydrophobic blocks have been widely used for the preparation of honeycomb-patterned porous films because they can gather at the interface between the solution and water droplets as well as to prevent water droplets from coalescing.[32] Shimomura et al. demonstrated that amphiphilic polymers can act as a second component to induce the formation of honeycomb structures from hydrophobic polymers.[39−42] Bolognesi et al. reported the fabrication of honeycomb films from an amphiphilic block copolymer containing a polystyrene block and a poly[9,9-di(2-(2-tetrahydropyranyl-oxy)hexyl)fluorene-*alt*-9,9-dioctylfluorene] block.[43] Moreover, the relationship between the composition of amphiphilic block copolymers and the morphologies of honeycomb films has obtained certain attention. For example, Saunders et al. discovered that increasing polymer hydrophobicity reduces water wettability at the air/polymer interface, which in turn decreases water droplet nucleation and thus influences the final pore size and regularity of the polymer films.[44] They suggested that the hydrophobic−hydrophilic balance of the polymer is important in stabilizing water droplets and preventing their coalescence. Wong et al. studied the influences of molecular weights of the hydrophilic block of polystyrene-*block*-poly(*N*,*N*-dimethylacrylamide) (PS-*b*-PDMA) and revealed that too-long PDMA block deteriorates the honeycomb structure.[45]

Although great advances have been made in understanding the relationship between polymer architectures and honeycomb film morphologies, a comprehensive study on the effects of the composition of amphiphilic block copolymers is very important, as it is crucial to the fabrication of large-area highly ordered honeycomb films with good reproducibility. Herein, we synthesized a series of amphiphilic polystyrene-based block copolymers, polystyrene-*block*-poly(*N*,*N*-dimethylaminoethly methacrylate) (PS-*b*-PDMAEMA) and polystyrene-*block*-poly(2-hydroxyethyl methacrylate) (PS-*b*-PHEMA), with different compositions by atom transfer radical polymerization (ATRP). The PDMAEMA block can be charged by quaternization, while the PHEMA block has reactive hydroxyl groups; and more importantly, PHEMA is more hydrophilic than PDMAEMA. These two block copolymers were used for preparing honeycomb films via the breath figure method. An empirical morphology diagram was concluded to reveal the relationship between block copolymer composition and film-forming ability. Moreover, the interfacial behaviors of these copolymers were discussed in detail. The results provide new insights into designing and screening polymers for honeycomb-patterned porous films.

EXPERIMENTAL SECTION

Materials. Styrene (St) was obtained from Sinopharm Chemical Reagent and distilled under reduced pressure before use. *N*,*N*-Dimethylaminoethyl methacrylate (DMAEMA) and 2-hydroxylethyl methacrylate (HEMA) were purchased from Aldrich and distilled under reduced pressure before use. The ATRP initiator, 1-phenylethyl bromide (1-PEBr), and *N*,*N*,*N*′,*N*″,*N*″-pentamethyldiethylenetriamine (PMDETA) were purchased from Aldrich and used without further purification. Copper(I) bromide (CuBr) was stirred in 2% glacial acetic acid aqueous solution overnight, filtered, and washed with absolute acetone under an argon blanket. Poly(ethylene terephthalate) (PET) film was kindly provided by Hangzhou Tape Factory and cleaned with acetone for 2 h before use. All other chemicals were analytical grade and used as received.

Synthesis of PS-Br Macroinitiators. ATRP of styrene was performed with a ratio of [M]/[I]/[PMDETA]/[CuBr] = 200−700/1/2/1. As a typical example, the synthesis of PS_{208} is described here. Styrene (20 mL, 174 mmol), 1-PEBr (60 μL, 0.44 mmol), and PMDETA (182 μL, 0.88 mmol) were added to a 100 mL round-bottomed flask with a magnetic stirrer. The flask was sealed and subjected to three freeze−pump−thaw cycles to remove dissolved oxygen. Then, CuBr (60 mg, 0.44 mmol) was added, and three more freeze−pump−thaw cycles were performed. The flask was then immediately immersed in an oil bath at 110 °C. The polymerization was stopped after a given period of time by quenching in liquid nitrogen. The mixture was then dissolved in a small amount of tetrahydrofuran (THF) and precipitated in methanol. The process was repeated three times to remove residual catalyst, ligand, and monomer. The final pure product was dried under reduced pressure overnight. The details of PS-Br are summarized in Table 1.

Table 1. Results of Polystyrene Macroinitiators Prepared via Atom Transfer Radical Polymerization

polymer[a]	[M]	time (min)	conv. (%)[b]	$M_{n,th}$[c]	$M_{n,GPC}$[d]	PDI[d]
PS_{73}	200	68	35.9	7500	7600	1.07
PS_{145}	200	132	70.7	14700	15200	1.07
PS_{208}	400	210	50.2	20900	21600	1.07
PS_{345}	400	305	84.1	35000	35900	1.23
PS_{456}	700	420	63.7	46400	47500	1.11

[a]Reaction conditions: [M]/[I]/[PMDETA]/[CuBr] = 200−700/1/2/1; 110 °C. [b]Calculated by the gravimetric method. Conv. (%) = W_p/W_{St}, where W_p and W_{St} are weights of the resultant polymer and styrene in feed, respectively. [c]Theoretical number-average molecular weight, $M_{n,th}$, was calculated according to $M_{n,th} = [St]_0 \times M_{St} \times conv./[I]_0 + M_I$, where M_{St} and M_I are molecular weights of styrene and the initiator, respectively. [d]GPC results measured using differential refractive index detection versus linear polystyrene standards.

Synthesis of PS-*b*-PDMAEMA. PS-*b*-PDMAEMA was synthesized by ATRP using a reported procedure.[46] Here the synthesis of PS_{208}-b1 is used as an example. PS_{208}-Br (1.08 g, 0.05 mmol), DMAEMA (252 μL, 1.5 mmol), PMDETA (21 μL, 0.1 mmol), and THF (5 mL) were added to a 50 mL round-bottomed flask with a magnetic stirrer. After degassed by three freeze−pump−thaw cycles, CuBr (7 mg, 0.05 mmol) was added, and three more freeze−pump−thaw cycles were performed. The flask was sealed and immersed in an oil bath at 50 °C while stirring. After 24 h, the polymerization was stopped by quenching in liquid nitrogen. The reaction mixture was precipitated by dropping the solution into methanol followed by filtration. The process was repeated three times. The final pure product was dried under reduced pressure overnight. Table 2 shows the details of the block copolymers.

Synthesis of PS-*b*-PHEMA. In a typical procedure (PS_{197}-*b*-$PHEMA_{18}$), PS_{197}−Br (0.51g, 0.025 mmol), HEMA (90 μL, 0.75 mmol), PMDETA (42 μL, 0.2 mmol), and chlorobenzene (5 mL) were put in a dry 50 mL Schlenk flask. The flask was

DOI: 10.1021/jp5119212
J. Phys. Chem. C 2015, 119, 1971−1979

Table 2. Ratios of Polymerization Degrees of PDMAEMA to PS of PS-*b*-PDMAEMA[a]

	PS_{73}	PS_{145}	PS_{208}	PS_{345}	PS_{456}
b0	0	0	0	0	0
b1	0.04	0.02	0.02	0.02	0.01
b2	0.08	0.04	0.06	0.05	0.02
b3	0.14	0.10	0.11	0.07	0.05
b4	0.21	0.18	0.16	0.12	0.09

[a]Calculated from ^{1}H NMR. For example, PS_{145}-b2 is PS_{145}-*b*-$PDMAEMA_6$. See Tables S1 and S2 in Supporting Information for details.

sealed and subjected to three freeze–pump–thaw cycles; then, a certain amount of CuBr (13 mg, 0.1 mmol) was added and three more freeze–pump–thaw cycles were performed. The polymerization was allowed to proceed in a preheated 80 °C oil bath. After 24 h, ^{1}H NMR analysis indicated that >50% of HEMA had been polymerized. The reaction was then stopped by quenching in liquid nitrogen. The mixture was then precipitated in methanol, and the process was repeated three times. The final pure product was dried under reduced pressure overnight. The details are summarized in Table S3 in the Supporting Information.

Film Preparation. Self-assembled honeycomb films were fabricated via a dynamic breath figure method under humid air flow. The polymers were dissolved in carbon disulfide at 1 or 2 mg/mL. An aliquot of 50 μL for each polymer solution was drop-cast onto a piece of PET substrate placed under a 2 L/min humid airflow (25 °C and ~80% RH). Owing to the condensation of water vapor on the solution surface during the evaporation of carbon disulfide, the transparent solution turned turbid rapidly. After solidification, the film was dried at room temperature.

Characterization. Proton nuclear magnetic resonance (^{1}H NMR) spectra of PS-*b*-PDMAEMA were recorded in $CDCl_3$ at room temperature on a Bruker (Advance DMX500) NMR instrument with tetramethylsilane (TMS) as the internal standard, and for PS-*b*-PHEMA, ^{1}H NMR spectra were acquired in DMSO-d_6 at 120 °C. Fourier transform infrared (FTIR) spectra were collected on a Nicolet FTIR/Nexus 470 spectrometer. Thirty-two scans were taken for each spectrum at a nominal resolution of 1 cm^{-1}. The molecular weight and molecular weight distribution were measured by a PL 220 gel permeation chromatography (GPC) instrument at 40 °C, which was equipped with a Waters 510 HPLC pump, three Waters Ultrastyragel columns (500, 103, and 105 Å), and a Waters 410 DRI detector. THF was used as the eluent at a flow rate of 1.0 mL min^{-1}. The calibration of the molecular weights was based on PS standards. A field-emission scanning electron microscope (FESEM, Sirion-100, FEI) was used to observe the surface morphologies of films after being sputtered with gold using an ion sputter JFC-1100. Interfacial tension was measured using the pendent drop technique by a Drop-Meter A-200 contact angle system (MAIST Vision Inspection & Measurement) at room temperature. The average values were calculated from at least three parallel measurements.

RESULTS AND DISCUSSION

Synthesis and Characterization of the Polymers. The ATRP of styrene was carried out under bulk conditions using 1-phenylethyl bromide as the initiator and PMDETA as the ligand in conjunction with CuBr at 110 °C.[47] It has been reported that the polymer can retain high bromide end-functionality via bulk ATRP.[48] In this work, polymerization time and feed ratios were controlled to synthesize well-designed polystyrene macroinitiators with different molecular weights. The results are summarized in Table 1. It can be seen that the molecular weights measured by GPC (Figure S1, Supporting Information) are close to the theoretical values calculated on the basis of monomer conversion, and the polymers have narrow molecular weight distributions (PDI = 1.1 to 1.2) even when the monomer conversion reaches as high as 85%.

Well-controlled amphiphilic block copolymers PS-*b*-PDMAEMA with a series of compositions were synthesized via ATRP under the same catalytic system using tetrahydrofuran as the solvent. The polymerization of each block can be tailored by controlling reaction time and feed ratios. Figure S2 in the Supporting Information shows a typical ^{1}H NMR spectrum of PS-*b*-PDMAEMA. A series of amphiphilic block copolymers PS-*b*-PDMAEMA initiated with the same macroinitiator were characterized by NMR and FT-IR (Figure 1 and

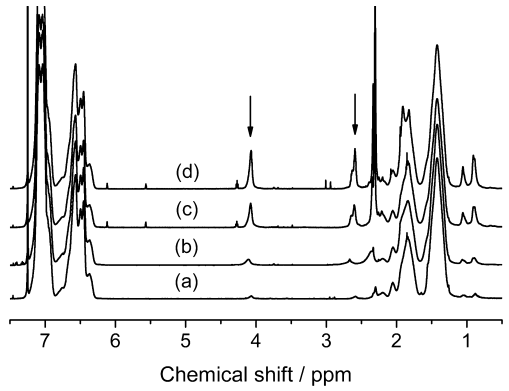

Figure 1. ^{1}H NMR spectra of (a) PS_{456}-*b*-$PDMAEMA_6$, (b) PS_{456}-*b*-$PDMAEMA_{11}$, (c) PS_{456}-*b*-$PDMAEMA_{22}$, and (d) PS_{456}-*b*-$PDMAEMA_{39}$.

Figure S3 in the Supporting Information). Peaks at 2.55 and 4.05 ppm are assigned to the protons of methylene on ester side chain in the PDMAEMA block. The peak around 1726 cm^{-1} is due to the carbonyl group in the PDMAEMA block. Results indicate that the characteristic peaks of PDMAEMA increase gradually with chain extension. The polymerization degree ratios of PDMAEMA to PS in the block copolymers can be calculated from the integral of the peaks at 2.55 and 4.05 ppm and that of the aromatic protons of PS at 6.40 to 7.20 ppm. Since the molecular weights of PS blocks have been measured by GPC, the polymerization degrees of the PDMAEMA blocks can be obtained (Table 2 and Table S1 in the Supporting Information). The molecular weights of the block copolymers measured by GPC are slightly smaller than those of the macroinitiator and decrease slightly with the polymerization degree of PDMAEMA block (Figure 2). This is due to the interaction of the polar PDMAEMA block with the GPC column, which leads to longer retention time and hence lowers molecular weights. With the increase in polymerization degree of PDMAEMA the molecular weight distribution increases slightly and remains in the range of 1.24 to 1.34 (Figure 2).

The synthesis of PS-*b*-PHEMA is similar to that of PS-*b*-PDMAEMA. The copolymerization was carried out in chlorobenzene at 80 °C, and about 50% yield was normally

DOI: 10.1021/jp5119212
J. Phys. Chem. C 2015, 119, 1971–1979

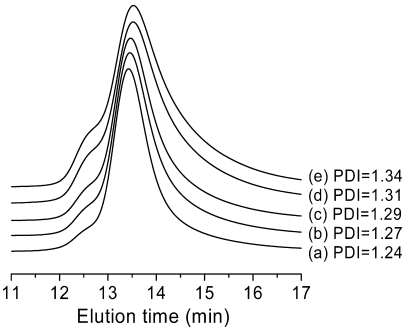

Figure 2. Typical GPC curves of PS-*b*-PDMAEMA. (a) PS_{345}, (b) PS_{345}-*b*-$PDMAEMA_6$, (c) PS_{345}-*b*-$PDMAEMA_{16}$, (d) PS_{345}-*b*-$PDMAEMA_{25}$, and (e) PS_{345}-*b*-$PDMAEMA_{43}$.

obtained after a polymerization time of 24 h. The composition of PS-*b*-PHEMA was characterized by GPC and ^{1}H NMR, as shown in Table S3 and Figure S4 in the Supporting Information. It can be seen from the results that well-controlled linear amphiphilic block copolymers have been synthesized, which are potential self-assembling materials for honeycomb-patterned porous films.

Fabrication of Honeycomb-Patterned Porous Films. Cost efficiency and simple operation of the breath figure method make it an attractive technique to prepare highly ordered porous films. However, highly ordered structure on a large scale with good reproducibility is very important for most of the applications. To this end, the polymer should possess robust film-forming ability. For amphiphilic block copolymer PS-*b*-PDMAEMA, a wide range of experimental conditions could be varied to fabricate honeycomb-patterned porous films. It has been demonstrated that solutions with high concentration may facilitate film formation.[49] Consequently, solutions with relatively low concentration (1 to 2 mg/mL) were used in this work to reveal the intrinsic film-forming ability of the polymers. When the concentration is 1 mg/mL (Figure 3), PS_{73} series that have the shortest PS block are not able to form regular honeycomb films regardless of the length of PDMAEMA block. A PS_{145}-based block copolymer with the least hydrophilic moieties can form highly ordered honeycomb structure. As the length of PS block increases, longer hydrophilic PDMAEMA block is endurable; that is, the fabrication window for ordered honeycomb films becomes wider for copolymers having longer PS block. For the PS_{456} series, which have the longest PS block in this study, all of the studied block copolymers are able to form ordered honeycomb films. Obviously, large area of highly ordered honeycomb films can be easily and highly reproducibly obtained when the polymerization degree ratio of hydrophilic PDMAEMA and hydrophobic PS blocks is at 0.01 to 0.02 (Figure S5 in the Supporting Information). It should be pointed out that in this work large-area ordering does not mean a single domain film. However, such multidomain feature is viable for many practical applications such as separation membranes and superhydrophobic surfaces. It should also be noted that, besides chemical composition, mechanical properties of polymers, such as elastic modulus, can also impact the formation of porous films.[50] However, the copolymers used in this work all possess a dominant PS chain that has the same molecular weight in each group and a very short hydrophilic block, which means that the

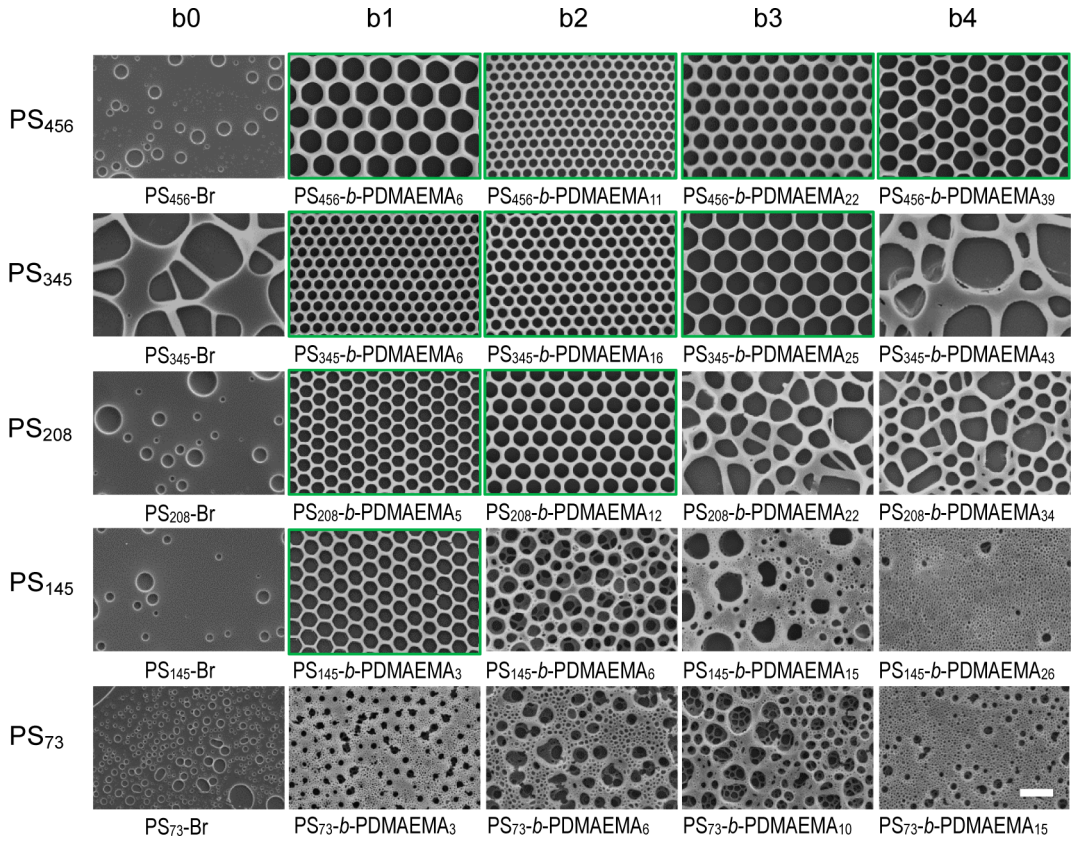

Figure 3. SEM images of films prepared from PS-*b*-PDMAEMA in CS_2 at 1 mg/mL. Images with green border mean ordered honeycomb films. The scale bar is 5 μm.

DOI: 10.1021/jp5119212
J. Phys. Chem. C 2015, 119, 1971−1979

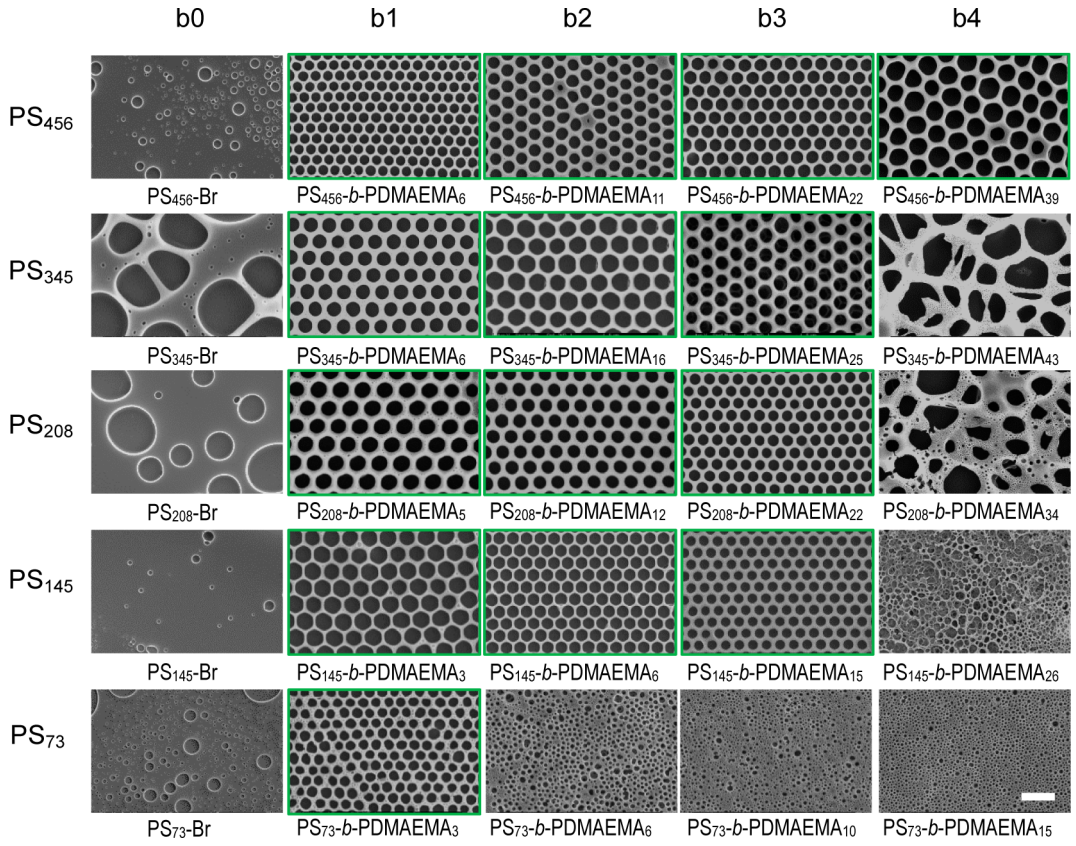

Figure 4. SEM images of films prepared from PS-*b*-PDMAEMA in CS_2 at 2 mg/mL. Images with green border mean ordered honeycomb films. The scale bar is 5 μm.

difference in the mechanical properties of these copolymers could be ignored to some extent. Therefore, it is reasonable to focus on the effects of chemical composition.

Film formation of the polymers at a relatively higher concentration of 2 mg/mL was also investigated. As shown in Figure 4, some polymers such as PS_{73}-b1, PS_{145}-b2, PS_{145}-b3, and PS_{208}-b3, which could not form regular films under low concentration (1 mg/mL), can be used to prepare ordered honeycomb films at 2 mg/mL. It is because higher polymer solution concentration results in a faster process of stabilizing water droplets.[51] As shown in Figures 3 and 4, block copolymers with excessively long PDMAEMA block (e.g., PS_{208}-b4) generate disordered films with wide pore size distribution, which is attributed to the coalescence of water droplets induced by the wetting and spreading of water on highly hydrophilic surface. Besides, considering the variation of pore size, we found that for polymers without long hydrophobic chain such as PS_{208} series, the diameters of the pores decrease with the polymerization degree of PDMAEMA. This is because more hydrophilic component lead to a greater ability to stabilize water droplets. Thus, the final film tends to possess larger specific surface area, resulting in smaller pore size. However, this rule seems invalid when hydrophobic PS chain is long enough. Once the molecular weight is above the critical entanglement molecular weight of PS ($M_n \approx 30\,000$ g/mol), some fluctuations appear, which may be due to the changed hydrodynamic volume of the polymers.

An empirical morphology diagram has been made to illustrate the dependence of film morphologies on the copolymer compositions on the basis of the results shown in Figures 3 and 4. In Figure 5, regularity of honeycomb-patterned

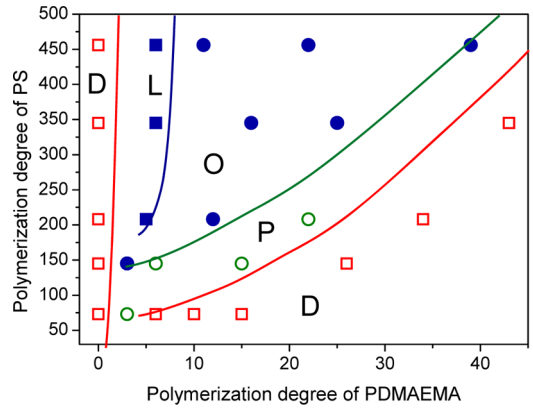

Figure 5. Dependence of the regularity of honeycomb films on the polymerization degrees of PS and PDMAEMA blocks in PS-*b*-PDMAEMA. **L** (filled square): large-area highly ordered; **O** (filled circle): ordered; **P** (hollow circle): partially ordered at high concentration; **D** (hollow square): disordered.

porous films prepared from PS-*b*-PDMAEMA with different compositions is represented using different symbols. There are three boundaries and four main zones, **L**, **O**, **P**, and **D**, which mean large-area ordered, ordered, partially ordered, and disordered films, respectively. The definition of these zones is based on the ratios of pore defects to the total pore number. Zone **L** indicates a ratio below 1%; the ratio in **O** is between 1 and 10%; for **P** it comes to 10 to 50%; and if the defective pores are in the main parts (>50%), it is defined as **D** (Figure S5 in the Supporting Information). The experiments were processed at least two times, and at least six films were involved in the

DOI: 10.1021/jp5119212
J. Phys. Chem. C 2015, 119, 1971−1979

calculations for each sample. In addition, the boundaries were determined approximately because of a finite number of samples of film-forming copolymers.

In the **L** zone, the length of hydrophilic block is short with a block length ratio between 0.01 and 0.02. These polymers, under our optimal experimental conditions, are able to form narrow pore-size distribution (with a CV <4%), large-area (>1 cm^2, which is dependent on the area of the cast solution), hexagonally patterned, almost defect-free (except domain boundaries), and highly reproducible honeycomb-patterned porous films. The main difference between **L** and **O** zones is that copolymers in the latter zone are more sensitive to other experimental conditions such as humidity. As a result, the reproducibility is slightly worse than the L zone, and defects may appear. The **P** zone is highly dependent on solution concentration, and ordered porous structure can be obtained at higher concentration. In this work, copolymers in this zone can form ordered films at 2 mg/mL but cannot at 1 mg/mL. This zone can be considered as a transitional region between ordering and disordering (**D**). Although this empirical morphology diagram depends on polymer concentration, it clearly reveals the general rule of chemical compositions of block copolymers that are able to form large-area highly ordered honeycomb films with good reproducibility.

Interfacial Tension Analysis. It has been accepted that polymers are able to precipitate at the interface of polymer solution and water to stabilize the water droplets. One of the keys to preparing ordered honeycomb-patterned films is to prevent water droplets from coalescence. Therefore, the interfacial tension between polymer solutions and water droplets plays a crucial role in determining the morphologies of honeycomb films. Fukuhira et al. studied the effects of interfacial tensions on the formation of honeycomb films by adding surfactants with different hydrophile−lipophile balance (HLB) values.[52] Effects of interfacial tensions of amphiphilic copolymers on honeycomb films were also discussed by Kojima et al.[41] They found that the HLB value and interfacial tension are important parameters affecting droplet stability. To elucidate the effects of the length of hydrophobic and hydrophilic blocks on the formation of honeycomb-patterned porous films, we measured interfacial tensions between water and the polymer solutions using the pendent drop technique. As previously mentioned, polymer concentration has a great influence on film formation. Figure 6 shows the results of interfacial tensions measured at concentrations ranging from 0 to 60 mg/mL. The interfacial tensions decrease with the increase in polymer concentrations and are lower than that of pure carbon disulfide (49.3 mN/m). At an initial concentration of 40 mg/mL, the interfacial tension can be lower than 20 mN/m. This result means that higher polymer concentration can effectively decrease the interfacial tension and thus stabilize condensed water droplets. Consequently, high concentration solution in a rational range can to some extent facilitate the formation of ordered honeycomb films.

It should be noted that the concentration will increase as the solvent evaporates during the film formation process. However, the initial polymer concentration plays a crucial role in determining the final structure of honeycomb films. It has been reported that a surface can be effectively reconstructed with as low as 0.3 wt % surface-active agents or groups in bulk.[53] In our system, it can be estimated that a critical concentration, C_c, of ∼0.1 mg/mL is enough for interfacial coverage by a monolayer of amphiphilic block copolymer for a

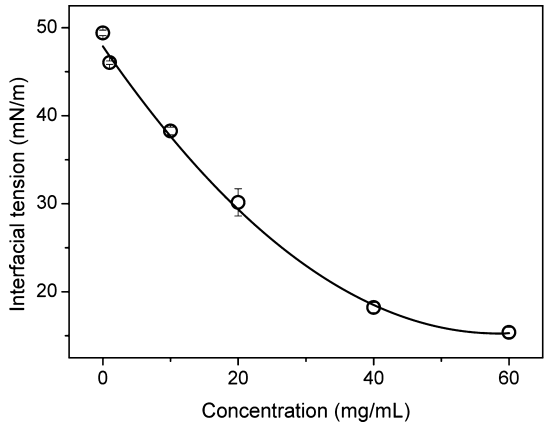

Figure 6. Interfacial tension between water and PS-*b*-PDMAEMA solutions in CS_2 with different concentrations. The polymer used is PS_{456}-*b*-$PDMAEMA_6$.

layer of hexagonally close-packed water droplets floated at the surface of cast solution with a thickness of about 50 μm

$$C_c = \frac{\frac{A_i / A_{mol}}{N_A} \times M_n}{V}$$

where A_i is the surface area of a water droplet, which is assumed as a round sphere with a diameter of 1 μm, A_{mol} is the cross-sectional area occupied by a single amphiphilic block copolymer at the interface (which is assumed to be ∼10 nm^2),[54] N_A is Avogadro's number, M_n is the molecular weight of the polymer (which is assumed to be 20 000 g/mol), and V is the volume of the cast solution with a thickness of ∼50 μm. Therefore, we measured interfacial tensions of 25 polymers with different chemical compositions (Table 2) dissolved in carbon disulfide at a concentration of 1 mg/mL, which is relatively low but higher than the critical concentration. The measurements were performed by slowly injecting the polymer solutions into deionized water. It is obvious that the interfacial tension decreases with the polymerization degree of PDMAEMA block (Figure 7). It is reasonable because these amphiphilic block copolymers may be considered as surfactants, which

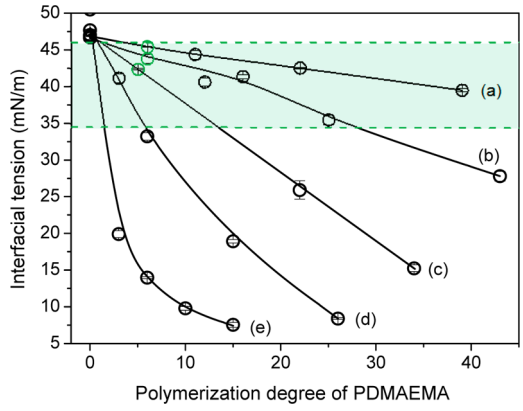

Figure 7. Interfacial tension between water and PS-*b*-PDMAEMA solutions in CS_2. The polymerization degrees of the PS blocks in the copolymers are (a) 456, (b) 345, (c) 208, (d) 145, and (e) 73. The polymer concentration is 1 mg/mL. Ordered honeycomb-patterned porous films located in the **L** and **O** zones were found to be formed from polymers with surface tensions in the green area. The interfacial tension between water and CS_2 was measured as 49.3 mN/m.

DOI: 10.1021/jp5119212
J. Phys. Chem. C 2015, 119, 1971−1979

could decrease interfacial tension between water and polymer solutions. As for macroinitiator PS-Br with different molecular weights, the interfacial tensions change little. However, the interfacial tensions of the amphiphilic block copolymers are totally different, which depends on the length of not only PDMAEMA block but also PS block. For PS_{456} series with the longest PS block, the chain extension by PDMAEMA makes the interfacial tension decrease gradually. When the hydrophobic PS block is shortened, the polymerization degree of PDMAEMA block would impact the interfacial tensions more effectively. Hence, PS_{73} series have the most dramatic decrease in interfacial tensions. Combined with film formation results shown in Figures 3 and 4, it can be concluded that an interfacial tension between 34.5 and 46.0 mN/m (between the dashed lines in Figure 7) is beneficial to the formation of ordered honeycomb films in zones **L** and **O** via the dynamic breath figure method for the PS-*b*-PDMAEMA system.

The changes in interfacial tensions can also be used to explain why block copolymers with large hydrophilic/hydrophobic block length ratios, that is, with low interfacial tensions, result in disordered films. The spreading coefficient, *S*, the work done in spreading water droplets over a unit area of polymer solution surface, was defined as[55]

$$S = \gamma_{sg} - (\gamma_{wg} + \gamma_{ws})$$

where γ_{sg}, γ_{wg}, and γ_{ws} are the interfacial tensions of polymer solution/gas, water/gas, and polymer solution/water, respectively. $S \geq 0$ means complete wetting and $S < 0$ indicates partial wetting. According to this equation, it is obvious that smaller γ_{ws} induces larger *S*. In our case, large spreading coefficient value indicates possible coalescence of water droplets, generating disordered films. Consequently, polymers with interfacial tensions lower than 34.5 mN/m are not able to form ordered honeycomb films in this work.

For comparison, a series of well-defined amphiphilic block copolymers PS_{197}-*b*-PHEMA were synthesized and utilized to prepare honeycomb-patterned porous films (Table S3 and Figure S6 in the Supporting Information). The polymerization degree of PHEMA block varies from 4 to 49. As a result of the large number of hydroxyl groups, PHEMA block is more hydrophilic than PDMAEMA. Correspondingly, polymers PS_{197}-*b*-$PHEMA_{18}$, PS_{197}-*b*-$PHEMA_{35}$, and PS_{197}-*b*-$PHEMA_{49}$ cannot fully dissolve in apolar solvent CS_2. All of the soluble block copolymers were employed to prepare honeycomb films. At 1 mg/mL, regular honeycomb films have been obtained from polymers PS_{197}-*b*-$PHEMA_4$ and PS_{197}-*b*-$PHEMA_8$. However, films from polymer PS_{197}-*b*-$PHEMA_{12}$ become less ordered (Figure S6d in the Supporting Information) under our experimental conditions, although its interfacial tension is similar to that of polymer PS_{197}-*b*-$PHEMA_4$, which is still in the range of 34.5−46.0 mN/m. As shown in Figure S7 in the Supporting Information, the interfacial tensions gradually decrease and then gradually rise with the increase in PHEMA block length. This could be attributed to the different aggregation state of polymer in solution. For polymers PS_{197}-*b*-$PHEMA_4$ and PS_{197}-*b*-$PHEMA_8$, a small amount of hydrophilic PHEMA component does not change the solubility of the block copolymers dramatically, which means that the block copolymers could exist as unimers in CS_2. As the PHEMA block length further increases, the interfacial tension increases slightly and then levels off, which could be explained by the aggregation state transition from unimers to reverse micelles.[56,57] It is well known that insoluble long hydrophilic block in apolar solvent tend to aggregate as a core and the corresponding hydrophobic block protect the core as a shell outside. For example, Eisenberg et al. reported that polystyrene-*block*-poly(acrylic acid) (PS-*b*-PAA) copolymer forms reverse micelles in toluene.[56] Therefore, amphiphilic block copolymers that are able to form reverse micelles can show different impacts on the morphologies of honeycomb films.

CONCLUSIONS

In summary, we synthesized a series of well-defined amphiphilic PS-*b*-PDMAEMA and PS-*b*-PHEMA diblock copolymers having various block length ratios and investigated the formation of honeycomb-patterned porous films by the breath figure method. We observed different zones showing large-area ordered (**L**), ordered (**O**), partially ordered (**P**), and disordered (**D**) films, which highly depend on the chemical compositions of the block copolymers. For PS-*b*-PDMAEMA, a polymerization degree ratio of PDMAEMA block to PS block between 0.01 and 0.02, which has an interfacial tension between 34.5 and 46.0 mN/m, is the best for the preparation of ordered honeycomb films in a reproducible way under a wide experimental window. For PS-*b*-PHEMA in which the PHEMA is more hydrophilic than PDMAEMA, the results are consistent with those of PS-*b*-PDMAEMA when the polymerization degree of PHEMA is smaller than 8; however, it forms reverse micelles and shows different self-assembling behaviors when the polymerization degree of PHEMA is larger than 12.

ASSOCIATED CONTENT

Supporting Information

GPC, NMR, and FT-IR results of polymers; images of typical honeycomb films; results of PS-*b*-PHEMA. This material is available free of charge via the Internet at http://pubs.acs.org.d

AUTHOR INFORMATION

Corresponding Author

*E-mail: lswan@zju.edu.cn. Tel: +86-571-87953763.

Notes

The authors declare no competing financial interest.

ACKNOWLEDGMENTS

Financial support from the National Natural Science Foundation of China (Grant No. 21374100 and 51173161) is gratefully acknowledged.

REFERENCES

(1) Connal, L. A.; Qiao, G. G. Preparation of porous poly(dimethylsiloxane)-based honeycomb materials with hierarchal surface features and their use as soft-lithography templates. *Adv. Mater.* **2006**, *18*, 3024−3028.

(2) Connal, L. A.; Franks, G. V.; Qiao, G. G. Photochromic, metal-absorbing honeycomb structures. *Langmuir* **2010**, *26*, 10397−10400.

(3) Galeotti, F.; Andicsova, A.; Yunus, S.; Botta, C. Precise surface patterning of silk fibroin films by breath figures. *Soft Matter* **2012**, *8*, 4815−4821.

(4) Ou, Y.; Zhu, L. W.; Xiao, W. D.; Yang, H. C.; Jiang, Q. J.; Li, X.; Lu, J. G.; Wan, L. S.; Xu, Z. K. Nonlithographic fabrication of nanostructured micropatterns via breath figures and solution growth. *J. Phys. Chem. C* **2014**, *118*, 4403−4409.

DOI: 10.1021/jp5119212
J. Phys. Chem. C 2015, 119, 1971−1979

(5) Erdogan, B.; Song, L. L.; Wilson, J. N.; Park, J. O.; Srinivasarao, M.; Bunz, U. H. F. Permanent bubble arrays from a cross-linked poly(para-phenyleneethynylene): Picoliter holes without microfabrication. *J. Am. Chem. Soc.* **2004**, *126*, 3678−3679.
(6) Li, X. F.; Zhang, L. A.; Wang, Y. X.; Yang, X. L.; Zhao, N.; Zhang, X. L.; Xu, J. A bottom-up approach to fabricate patterned surfaces with asymmetrical TiO_2 microparticles trapped in the holes of honeycomb-like polymer film. *J. Am. Chem. Soc.* **2011**, *133*, 3736−3739.
(7) Yabu, H.; Shimomura, M. Single-step fabrication of transparent superhydrophobic porous polymer films. *Chem. Mater.* **2005**, *17*, 5231−5234.
(8) Wan, L. S.; Li, J. W.; Ke, B. B.; Xu, Z. K. Ordered microporous membranes templated by breath figures for size-selective separation. *J. Am. Chem. Soc.* **2012**, *134*, 95−98.
(9) Du, C.; Zhang, A. J.; Bai, H.; Li, L. Robust microsieves with excellent solvent resistance: Cross-linkage of perforated polymer films with honeycomb structure. *ACS Macro Lett.* **2013**, *2*, 27−30.
(10) Zhang, C. Y.; Wang, X. F.; Min, K.; Lee, D.; Wei, C.; Schulhauser, H.; Gao, H. F. Developing porous honeycomb films using miktoarm star copolymers and exploring their application in particle separation. *Macromol. Rapid Commun.* **2014**, *35*, 221−227.
(11) Ou, Y.; Lv, C. J.; Yu, W.; Mao, Z. W.; Wan, L. S.; Xu, Z. K. Fabrication of perforated isoporous membranes via a transfer-free strategy: Enabling high-resolution separation of cells. *ACS Appl. Mater. Interfaces* **2014**, *6*, 2400−22407.
(12) Chen, P. C.; Wan, L. S.; Ke, B. B.; Xu, Z. K. Honeycomb-patterned film segregated with phenylboronic acid for glucose sensing. *Langmuir* **2011**, *27*, 12597−12605.
(13) Zhang, Y.; Wang, C. Micropatterning of proteins on 3D porous polymer films fabricated by using the breath-figure method. *Adv. Mater.* **2007**, *19*, 913−916.
(14) Yin, S. Y.; Goldovsky, Y.; Herzberg, M.; Liu, L.; Sun, H.; Zhang, Y. Y.; Meng, F. B.; Cao, X. B.; Sun, D. D.; Chen, H. Y.; Kushmaro, A.; Chen, X. D. Functional free-standing graphene honeycomb films. *Adv. Funct. Mater.* **2013**, *23*, 2972−2978.
(15) Wang, Y. R.; Liu, Y.; Li, G. H.; Hao, J. C. Porphyrin-based honeycomb films and their antibacterial activity. *Langmuir* **2014**, *30*, 6419−6426.
(16) Jiang, X. L.; Zhang, T. Z.; He, S. Y.; Ling, J. J.; Gu, N.; Zhang, Y.; Zhou, X. F.; Wang, X.; Cheng, L. Bacterial adhesion on honeycomb-structured poly(L-lactic acid) surface with Ag nanoparticles. *J. Biomed. Nanotechnol.* **2012**, *8*, 791−799.
(17) Lee, S. H.; Kim, H. W.; Hwang, J. O.; Lee, W. J.; Kwon, J.; Bielawski, C. W.; Ruoff, R. S.; Kim, S. O. Three-dimensional self-assembly of graphene oxide platelets into mechanically flexible macroporous carbon films. *Angew. Chem., Int. Ed.* **2010**, *49*, 10084−10088.
(18) Wang, J.; Wang, C. F.; Shen, H. X.; Chen, S. Quantum-dot-embedded ionomer-derived films with ordered honeycomb structures via breath figures. *Chem. Commun.* **2010**, *46*, 7376−7378.
(19) Yin, S. Y.; Zhang, Y. Y.; Kong, J. H.; Zou, C. J.; Li, C. M.; Lu, X. H.; Ma, J.; Boey, F. Y. C.; Chen, X. D. Assembly of graphene sheets into hierarchical structures for high-performance energy storage. *ACS Nano* **2011**, *5*, 3831−3838.
(20) Heng, L. P.; Qin, W.; Chen, S. J.; Hu, R. R.; Li, J.; Zhao, N.; Wang, S. T.; Tang, B. Z.; Jiang, L. Fabrication of small organic luminogens honeycomb-structured films with aggregation-induced emission features. *J. Mater. Chem.* **2012**, *22*, 15869−15873.
(21) Widawski, G.; Rawiso, M.; Francois, B. Self-organized honeycomb morphology of star-polymer polystyrene films. *Nature* **1994**, *369*, 387−389.
(22) Wan, L. S.; Zhu, L. W.; Ou, Y.; Xu, Z. K. Multiple interfaces in self-assembled breath figures. *Chem. Commun.* **2014**, *50*, 4024−4039.
(23) Munoz-Bonilla, A.; Fernandez-Garcia, M.; Rodriguez-Hernandez, J. Towards hierarchically ordered functional porous polymeric surfaces prepared by the breath figures approach. *Prog. Polym. Sci.* **2014**, *39*, 510−554.
(24) Bai, H.; Du, C.; Zhang, A. J.; Li, L. Breath figure arrays: Unconventional fabrications, functionalizations, and applications. *Angew. Chem., Int. Ed.* **2013**, *52*, 12240−12255.
(25) Bunz, U. H. F. Breath figures as a dynamic templating method for polymers and nanomaterials. *Adv. Mater.* **2006**, *18*, 973−989.
(26) Stenzel-Rosenbaum, M. H.; Davis, T. P.; Fane, A. G.; Chen, V. Porous polymer films and honeycomb structures made by the self-organization of well-defined macromolecular structures created by living radical polymerization techniques. *Angew. Chem., Int. Ed.* **2001**, *40*, 3428−3432.
(27) Stenzel, M. H.; Davis, T. P.; Fane, A. G. Honeycomb structured porous films prepared from carbohydrate based polymers synthesized via the raft process. *J. Mater. Chem.* **2003**, *13*, 2090−2097.
(28) Hernandez-Guerrero, M.; Davis, T. P.; Barner-Kowollik, C.; Stenzel, M. H. Polystyrene comb polymers built on cellulose or poly(styrene-co-2-hydroxyethylmethacrylate) backbones as substrates for the preparation of structured honeycomb films. *Eur. Polym. J.* **2005**, *41*, 2264−2277.
(29) Jenekhe, S. A.; Chen, X. L. Self-assembly of ordered microporous materials from rod-coil block copolymers. *Science* **1999**, *283*, 372−375.
(30) Hayakawa, T.; Horiuchi, S. From angstroms to micrometers: Self-organized hierarchical structure within a polymer film. *Angew. Chem., Int. Ed.* **2003**, *42*, 2285−2289.
(31) Cheng, C. X.; Tian, Y.; Shi, Y. Q.; Tang, R. P.; Xi, F. Porous polymer films and honeycomb structures based on amphiphilic dendronized block copolymers. *Langmuir* **2005**, *21*, 6576−6581.
(32) Hayakawa, T.; Kouketsu, T.; Kakimoto, M.; Yokoyama, H.; Horiuchi, S. Patterned surfaces in self-organized block copolymer films with hexagonally ordered microporous structures. *Macromol. Res.* **2006**, *14*, 52−58.
(33) Kadla, J. F.; Asfour, F. H.; Bar-Nir, B. Micropatterned thin film honeycomb materials from regiospecifically modified cellulose. *Biomacromolecules* **2007**, *8*, 161−165.
(34) Li, X. Y.; Zhao, Q. L.; Xu, T. T.; Huang, J.; Wei, L. H.; Ma, Z. Highly ordered microporous polystyrene-*b*-poly(acrylic acid) films: Study on the influencing factors in their fabrication via a static breath-figure method. *Eur. Polym. J.* **2014**, *50*, 135−141.
(35) Peng, J.; Han, Y. C.; Yang, Y. M.; Li, B. Y. The influencing factors on the macroporous formation in polymer films by water droplet templating. *Polymer* **2004**, *45*, 447−452.
(36) Li, L.; Li, J. A.; Zhong, Y. W.; Chen, C. K.; Ben, Y.; Gong, J. L.; Ma, Z. Formation of ceramic microstructures: Honeycomb patterned polymer films as structure-directing agent. *J. Mater. Chem.* **2010**, *20*, 5446−5453.
(37) Billon, L.; Manguian, M.; Pellerin, V.; Joubert, M.; Eterradossi, O.; Garay, H. Tailoring highly ordered honeycomb films based on ionomer macromolecules by the bottom-up approach. *Macromolecules* **2009**, *42*, 345−356.
(38) Zhu, L. W.; Yang, W.; Ou, Y.; Wan, L. S.; Xu, Z. K. Synthesis of polystyrene with cyclic, ionized and neutralized end groups and the self-assemblies templated by breath figures. *Polym. Chem.* **2014**, *5*, 3666−3672.
(39) Yabu, H.; Shimomura, M. Mesoscale pincushions, microrings, and microdots prepared by heating and peeling of self-organized honeycomb-patterned films deposited on a solid substrate. *Langmuir* **2006**, *22*, 4992−4997.
(40) Yabu, H.; Hirai, Y.; Shimomura, M. Electroless plating of honeycomb and pincushion polymer films prepared by self-organization. *Langmuir* **2006**, *22*, 9760−9764.
(41) Kojima, M.; Hirai, Y.; Yabu, H.; Shimomura, M. The effects of interfacial tensions of amphiphilic copolymers on honeycomb-patterned films. *Polym. J.* **2009**, *41*, 667−671.
(42) Yabu, H.; Hirai, Y.; Kojima, M.; Shimomura, M. Simple fabrication of honeycomb- and pincushion-structured films containing thermoresponsive polymers and their surface wettability. *Chem. Mater.* **2009**, *21*, 1787−1789.
(43) Bolognesi, A.; Galeotti, F.; Giovanella, U.; Bertini, F.; Yunus, S. Nanophase separation in polystyrene-polyfluorene block copolymers

DOI: 10.1021/jp5119212
J. Phys. Chem. C 2015, 119, 1971−1979

thin films prepared through the breath figure procedure. *Langmuir* **2009**, *25*, 5333−5338.
(44) Saunders, A. E.; Dickson, J. L.; Shah, P. S.; Lee, M. Y.; Lim, K. T.; Johnston, K. P.; Korgel, B. A. Breath figure templated self-assembly of porous diblock copolymer films. *Phys. Rev. E* **2006**, *73*, 7.
(45) Wong, K. H.; Davis, T. P.; Bamer-Kowollik, C.; Stenzel, M. H. Honeycomb structured porous films from amphiphilic block copolymers prepared via raft polymerization. *Polymer* **2007**, *48*, 4950−4965.
(46) Zhang, X.; Xia, J. H.; Matyjaszewski, K. Controlled/″living″ radical polymerization of 2-(dimethylamino)ethyl methacrylate. *Macromolecules* **1998**, *31*, 5167−5169.
(47) Ke, B. B.; Wan, L. S.; Zhang, W. X.; Xu, Z. K. Controlled synthesis of linear and comb-like glycopolymers for preparation of honeycomb-patterned films. *Polymer* **2010**, *51*, 2168−2176.
(48) Hong, S. C.; Lutz, J. F.; Inoue, Y.; Strissel, C.; Nuyken, O.; Matyjaszewski, K. Use of an immobilized/soluble hybrid atrp catalyst system for the preparation of block copolymers, random copolymers, and polymers with high degree of chain end functionality. *Macromolecules* **2003**, *36*, 1075−1082.
(49) Sanz de Leon, A.; Rodriguez-Hernandez, J.; Cortajarena, A. L. Honeycomb patterned surfaces functionalized with polypeptide sequences for recognition and selective bacterial adhesion. *Biomaterials* **2013**, *34*, 1453−1460.
(50) Zhang, Z.; Hughes, T. C.; Gurr, P. A.; Blencowe, A.; Hao, X.; Qiao, G. G. Influence of polymer elasticity on the formation of non-cracking honeycomb films. *Adv. Mater.* **2012**, *24*, 4327−4330.
(51) Liu, W. Y.; Liu, R. G.; Li, Y. X.; Wang, W.; Ma, L.; Wu, M.; Huang, Y. Self-organized ordered microporous thin films from grafting copolymers. *Polymer* **2009**, *50*, 2716−2726.
(52) Fukuhira, Y.; Yabu, H.; Ijiro, K.; Shimomura, M. Interfacial tension governs the formation of self-organized honeycomb-patterned polymer films. *Soft Matter* **2009**, *5*, 2037−2041.
(53) Yabu, H.; Jia, R.; Matsuo, Y.; Ijiro, K.; Yamamoto, S.-a.; Nishino, F.; Takaki, T.; Kuwahara, M.; Shimomura, M. Preparation of highly oriented nano-pit arrays by thermal shrinking of honeycomb-patterned polymer films. *Adv. Mater.* **2008**, *20*, 4200−4204.
(54) Tsujii, Y.; Ohno, K.; Yamamoto, S.; Goto, A.; Fukuda, T. Structure and properties of high-density polymer brushes prepared by surface-initiated living radical polymerization. *Adv. Polym. Sci.* **2006**, *197*, 1−45.
(55) Wan, L. S.; Ke, B. B.; Zhang, J.; Xu, Z. K. Pore shape of honeycomb-patterned films: Modulation and interfacial behavior. *J. Phys. Chem. B* **2012**, *116*, 40−47.
(56) Khougaz, K.; Zhong, X. F.; Eisenberg, A. Aggregation and critical micelle concentrations of polystyrene-b-poly(sodium acrylate) and polystyrene-b-poly(acrylic acid) micelles in organic media. *Macromolecules* **1996**, *29*, 3937−3949.
(57) Nakano, M.; Deguchi, M.; Matsumoto, K.; Matsuoka, H.; Yamaoka, H. Self-assembly of poly(1,1-diethylsilabutane)-block-poly-(2-hydroxyethyl methacrylate) block copolymer. 1. Micelle formation and micelle-unimer-reversed micelle transition by solvent composition. *Macromolecules* **1999**, *32*, 7437−7443.

DOI: 10.1021/jp5119212
J. Phys. Chem. C 2015, 119, 1971−1979